

Residual Drift Mitigation in Concentrically Braced Frames using Hybrid Braces

M.S. Pandikkadavath & Dipti Ranjan Sahoo

Department of Civil Engineering, Indian Institute of Technology Delhi.

ABSTRACT: Conventional Concentrically Braced Frames (CBFs) with buckling-type braces (BTBs) can contribute substantial lateral stiffness to framed structures and hence, are widely adopted in structures located in seismically active regions. However, the inferior asymmetric hysteretic response and vulnerability to brace fracture at higher drift levels are major concerns associated with BTBs. On the other hand, Buckling-Restrained Braces (BRBs) possessing yielding capacity in tension as well as in compression have nearly symmetric hysteretic response. The main limitation of Buckling-Restrained Braced Frames (BRBFs) is the higher drift response when compared to CBFs. This may adversely affect the retrofitting and reusability of the structures after a seismic event. A hybrid brace that can maintain the symmetric hysteresis (similar to that of BRBs) along with increased stiffness (similar to that of BTBs) can give out the preferred hysteresis. This can be achieved by incorporating a BTB as an elastic segment and a short-length BRB (SLBRB) in series as a single hybrid brace (HB). The seismic behaviour of such Hybrid Braced Frames (HBFs) for two different heights (3 and 6 storey) has been investigated using nonlinear static and dynamic analyses. The design of HBFs has been carried out for two different values of response reduction factor (R), namely, for $R = 7$ and 8. Dynamic analyses has been conducted for twenty selected ground motion representing the Design Basis Earthquake (DBE) hazard level. The seismic performance of HBFs has been compared with equivalent CBFs and BRBFs. Results showed that HBFs have significantly reduced residual drifts compared to the BRBFs.

Keywords: braced frame; nonlinear modelling; seismic design; seismic analysis; drift

1 INTRODUCTION

Buckling Restrained Braced Frames (BRBFs) are relatively new type of concentrically braced frames (CBFs). BRBFs have received wide acceptance for the seismic proofing of framed structures located in seismically active zones. The prevention of brace fracture and the desirable balanced hysteresis of Buckling Restrained Braces (BRBs) make them preferable over typical Buckling-Type Braces (BTBs). The BRBs consists of a metallic core plate (often made of steel) and a buckling inhibiting encasement (usually hollow steel sections) filled with concrete or mortar. A de-bonding agent all around the core plate with allowance for Poisson effect will ensure the minimized shear interaction between the core plate and the surrounding concrete/mortar confinement. Fig. 1 represents the schematic representation of BRB with its cross sectional details. The buckling prevention by the encasement allows the core plate to yield in compression as well. This give out a smaller cross-sectional area requirement for BRBs and hence results in a reduced stiffness to the overall system. This abatement in the stiffness effectively increases drift demands associated with BRBFs (Sabelli 2000; Sabelli et al. 2003). The hike in drift demands can adversely affect the retro-fitting and reusability of the BRBFs after the earthquake. On the other hand, CBFs with BTBs possess sufficient stiffness to limit drift demands within the desirable range. However, the probable brace fracture at higher seismic demands and the inferior asymmetric hysteresis associated with BTBs may damage the gravity load resisting components of the frame system. A brace possessing adequate stiffness comparable to BTBs and stable balanced hysteresis as that of BRBs can result in a very acceptable response. This study investigate the possibility of such a hybrid brace (HB) in CBFs to improve its seismic performance.

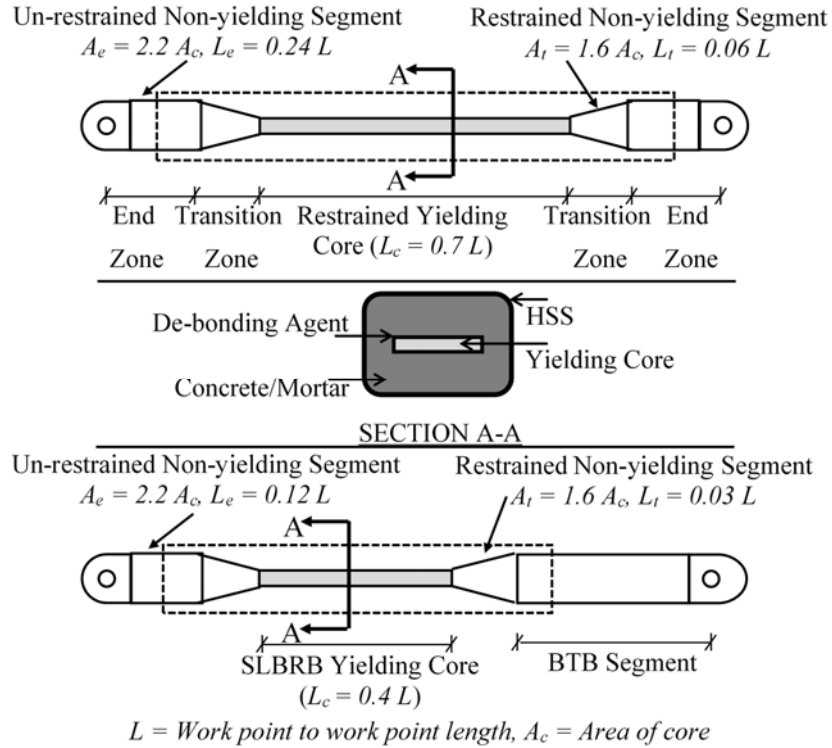


Fig. 1. Typical Buckling Restrained Brace (BRB) and proposed Hybrid Brace (HB) with cross section details

The metallic core plate of BRBs have a central yielding core region for a major length followed by a non-yielding transition and end zones respectively towards the end on either side. The yieldable core region mostly possess a length of about 70% of the total work point to work point length (Merritt et al. 2003). The remaining length will be shared between restrained transition zone (6% of work point to work point length) and un-restrained end zones (24% of work point to work point length). The cross-sectional area for transition zone and end zones will be about 160% and 220% of core the area (A_c) respectively as shown in Fig. 1 (Sahoo & Chao 2010). For the proposed HB, a yielding core length of 40% of the total length between work points were considered. This proportion was selected on the basis that the assumed yielding core length can meet higher mode buckling yield length requirements. Past studies reported that for higher mode compression yielding, a single wavelet may require 8 to 12 times the core plate thickness, t_c (Wu et al. 2014). By equating tension yield strength to compression yield strength (Euler buckling formulae), the compression yielding mode and hence the minimum core yield length can be found. The relationship between t_c and mode number for different brace lengths is shown in Fig. 2. For the yielding core a yield stress of 248 MPa and an over strength of 1.3 was considered (Pandikkadavath & Sahoo 2010 and Sahoo & Chao 2010). For this study a yielding core length of 40% of work point to work point length satisfies the higher mode compression yielding requirement for all the braces. The scope of this study was mainly limited to evaluating the drift demands. The incorporation of reduced yielding core length was done by taking HB as a combination of a Short length BRB (SLBRB) for the lower portion and the remaining top segment with elastic BTBs in series. The connection between the SLRBRB and the BTB segment is assumed to be continuous without any lag effect. During the in-elastic action the SLBRB segment can undergo symmetric hysteresis to dissipate the energy while the BTB segment remains elastic and provide adequate stiffness to limit the drift demand. The seismic response of the steel hybrid braced frame (HBF) fitted with the proposed HB and its response comparison with equivalent BRBFs and HBFs are presented in the following sections.

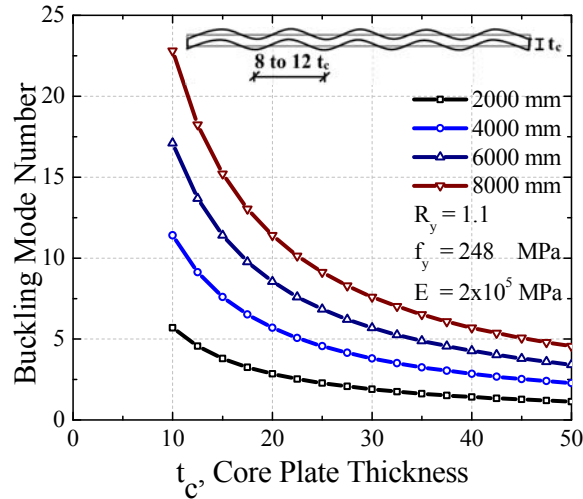


Fig. 2. Relation between core plate thickness and compression yielding mode number

2 BUILDING MODELS

Two different steel buildings 3 and 6 storey were considered for the analytical investigations. All the buildings adopted pinned end inverted-V configuration for the braces. The centre to centre plan dimension of 3-storey building was 36.56 m (four bays at 9.14 m) by 54.84 m (6 bays at 9.14 m). The total height of the same building was 11.88 m (3 storeys at 3.96 m each). It consists of four braced bays along each direction symmetrically placed along the periphery. Fig. 3 shows the plan of the 3 storey building and elevations of the representative braced bays. The 6 storey building had a total height of 25.29 m (5.49 m at the bottom storey and 3.96 m each for the remaining floors). The plan dimension was 54.84 m by 54.84 m (six bays at 9.14 m along both direction) with 0.6 m projections all around. For the 6 storey building six braced bays were symmetrically placed on the periphery along each direction. All the interior bays were gravity load bearing type. For the 3-storey building, one of the brace bay along the shorter plan direction and for 6-storey building a braced bay at extreme corner were selected for the design and analysis. Fig. 4 shows the dimensional details along with braced bay details of the 6-storey building.

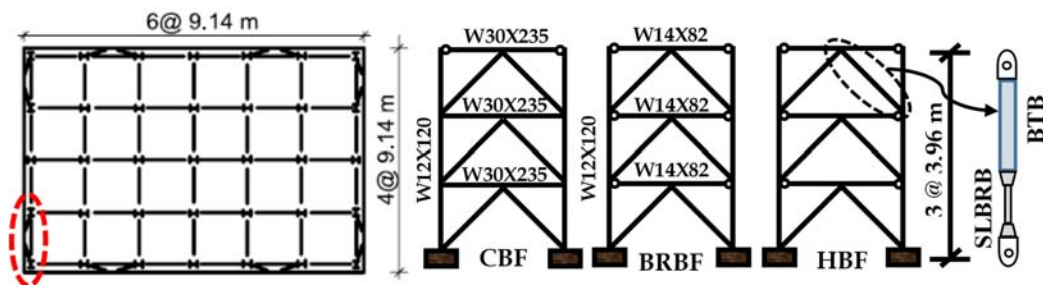


Fig. 3. Plan of the 3-storey building with elevations of CBF, BRBF and HBF systems

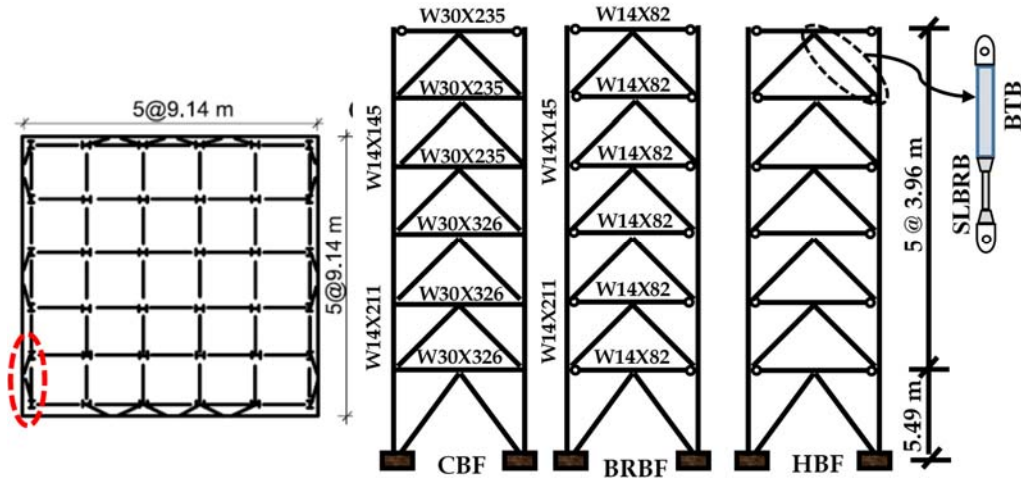


Figure 4. Plan of the 6-storey building with elevation of CBF, BRBF and HBF systems

2.1 Design Methodology

The buildings were designed as per the current U.S. codes (ASCE/SEI 7-10, 2010; AISC/ANSI 341-10, 2010 & AISC/ANSI 360-10, 2010). The buildings were assumed to be located on deep stiff soil (site class D). The spectral response acceleration (5% critical damping) value for 0.2 s (S_{DS}) and 1 s (S_{D1}) were 1.393g and 0.77g respectively for all the buildings considered. Different values of response reduction factor (R) was used for building depending on the evaluation requirements. CBF with BTB used an R value of 6, hence it is designated as 3VCBFR6 and 6VCBFR6 for 3 and 6 storey frames respectively. For BRBF and HBF, two values of R (7 and 8) were used, subsequently these frames considered for the analysis were named as 3VBRBF7, 3VBRBF8, 6VBRBF7, 6VBRBF8, 3VHBF7, 3VHBF8, 6VHBF7 and 6VHBF8 with respect to their number of stories. The approximate time period (C_T) for 3VCBFR6 was 0.31 s. C_T for all other 3-storey frames were found to be 0.47 s. The C_T of all 6-storey frames except for 6VCBFR6 were 0.84 s and that of 6VCBFR6 was 0.56 s. Considering an importance factor, $I=1$ for all the buildings the seismic response co-efficient (C_S) obtained were 0.23 for CBFs, 0.17 for BRBFs and HBFs with $R=8$, and 0.2 for BRBFs and HBFs with $R=7$ in respective order. The seismic weight of the 3-storey building was 26983 kN and that for 6-storey building was 56065 kN. The vertical lateral load distribution over the height was distributed as per ASCE/SEI 7-10 (2010) recommendations. A live load of 2 kN/m² on roof and 3 kN/m² on the floors were considered for all the buildings.

2.2 Design of Braces and Frame Members

The brace forces were obtained by resolving the storey shear in the direction of respective braces. All the braces were assumed to be pinned at their ends. For CBFs all the BTBs are designed as HSS considering the buckling strength in compression. The width to thickness ratio of BTBs were kept within the range of highly ductile members. The effective length factor K , was taken as 0.85 assuming out of plane buckling. The yield strength (f_y) of 317 MPa and an over strength factor (R_y) of 1.1 was assumed for the design of BTBs (Chao et al. 2012). The post buckling strength of BTBs were taken as 0.3 times the buckling strength of the BTBs. For the BRBs a yield strength (f_y) of 248 MPa with R_y of 1.3 was considered. The tension strength adjustment factor (ω) of 1.4 and a compression strength adjustment factor (β) of 1.1 was assumed for the design of BRBs (Sahoo & Chao 2010). The maximum tensile stress (F_T) developed in the BRB were $\omega f_y R_y$ and the maximum compressive stress (F_C) developed in the BRB were $\beta \omega f_y R_y$. For the HB the parameters of SLBRBs were kept same as that of BRBs (Pandikkadavath & Sahoo 2014). For the elastic segment, the HSS sections with a yielding strength of 1.5 times the ultimate strength of SLBRBs was taken. Table 1 summarises the cross section details of braces for different frames. For all the stories the elastic BTBs for 3VHBF8 and 3VHBF7 were taken as HSS10X10X1/2. The elastic BTB for 6VHBF8 and 6VHBF7 were considered as HSS12X12X1/2 for all the storeys.

The beams and columns of the frames were designed as frame members. The beams in all frames were designed for maximum unbalanced forces developed in brace pairs due to difference in ultimate tension and compression forces. The beam column joints of CBFs were taken as fixed at all stories except on the roof. On the top floor of CBF and in all the floors of BRBFs and HBFs the beam-column connections were taken as pinned (Fahnestock et al. 2007). The columns were designed as fixed at bottom at continuous till the top floor. Columns were designed as axial members considering maximum axial load from the code prescribed load combinations. Fig. 3 and 4 gives the details of frame member components. For BRBFs and HBFs identical non-yielding components were considered.

Table 1. Details of brace cross-section used in this study

3-Storey Frame					
	3VCBFR6 BTB	3VBRBFR8 BRB (mm ²)	3VBRBFR7 BRB (mm ²)	3VHBFR8 SLBRB (mm ²)	3VHBFR7 SLBRB (mm ²)
3 rd Storey	HSS5X5X3/8	2069	2364	2069	2364
2 nd Storey	HSS6X6X1/2	3103	3546	3103	3546
1 st Storey	HSS6X6X1/2	3723	4255	3723	4255
6-Storey Frame					
	6VCBFR6 BTB	6VBRBFR8 BRB (mm ²)	6VBRBFR7 BRB (mm ²)	6VHBFR8 SLBRB (mm ²)	6VHBFR7 SLBRB (mm ²)
6 th Storey	HSS5X5X5/16	1243	1419	1243	1419
5 th Storey	HSS6X6X1/2	1921	2195	1921	2195
4 th Storey	HSS6X6X1/2	2599	2971	2599	2971
3 rd Storey	HSS7X7X1/2	3101	3544	3101	3544
2 nd Storey	HSS7X7X1/2	3433	3924	3433	3924
1 st Storey	HSS8X8X1/2	4252	4859	4252	4859

3 ANALYTICAL INVESTIGATIONS

The non-linear static and dynamic analysis of all frames were carried out using PERFORM-3D (2013) software. For the beam and column members standard sections were chosen from the inbuilt library as per design requirements. Bi-linear lumped plasticity model as per FEMA 356 (2000) was assigned for the members. For the beams, flexural hinges at expected locations of maximum bending moments were assigned. For the columns, flexure as well as axial load-moment interaction hinges were assigned at the salient locations. Connection panel zones for beam-column joints were modelled by taking their respective dimensions and yield strengths for all the frames.

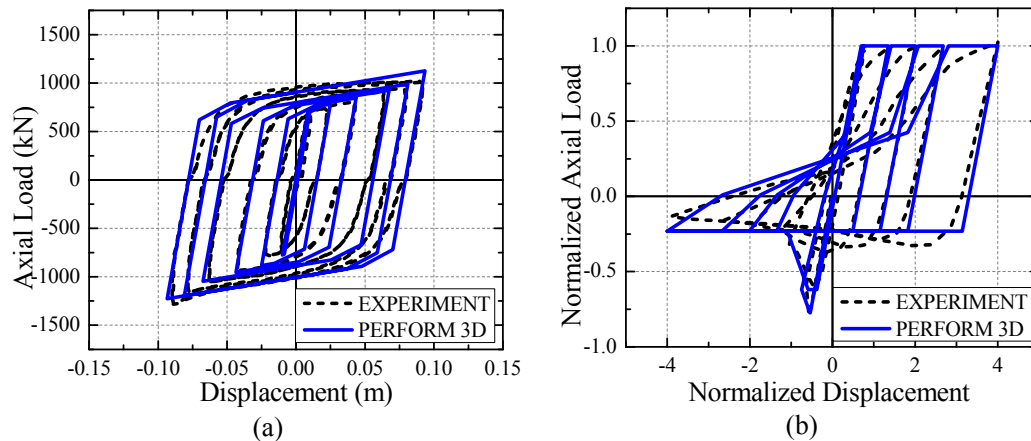


Figure 5. (a) Hysteresis model for BRB, (b) Hysteresis model for BTB

The BTBs were modelled using inelastic buckling type material and the cross sectional details were assigned as inelastic beam fibre sections. For BRBs standard pre-defined functions were used. A post yield stiffness of 3% was considered for both the BRBs and SLBRBs. For the HB 40% of total length between work points ends had been assigned as the yielding core length of SLBRBs. The elastic transition and end zones for SLBRBs were assigned as 3% and 12% of total work point lengths respectively (Refer Fig. 1). The cross-sections of the same were 160% and 220% of the central yielding zone area (A_c) respectively. In order to represent the hysteresis both isotropic and kinematic models were considered. The remaining portion was assigned with BTB with lumped plasticity at 0.25, 0.5 and 0.75 proportionate length of elastic BTB segment of HB. The analysis result showed that in all the cases the BTB part in all HBs remained elastic while the SLBRBs dissipated the energy in the preferred way. The software in-built hysteresis model of BRBs and BTBs were matched with experimental results (Merritt et al. 2003 and Shaback & Brown 2003). The adopted hysteretic models for BRBs and BTBs are shown in Fig. 5 (a) & (b). To account for the eccentricity of loading on the braced frames a gravity P- Δ column was modelled in all the frames. The gravity column was pinned at the base and continuous to the top (Sahoo & Chao 2010). The property of the gravity column is chosen considering the sum of properties of interior columns assuming predominant bending was about the weak axis. The gravity column is connected to brace frame by a rigid link with moment release at the joints. This will ensure that the rigid connection will transfer only axial load with same drift along the same floor. The scope of the investigation is limited to limit drift response up to collapse prevention. Hence nonlinear time-history analysis for the selected 20 SAC ground motions comes under design basis earthquake (DBE hazard level), having 10% probability in 50 years was used (Somerville et al. 1997). Fig. 6 shows the response spectrum of 20 DBE level earthquake and its average along with design response spectra. Rayleigh damping of 2% was used for the non-linear time history (NTH) analysis.

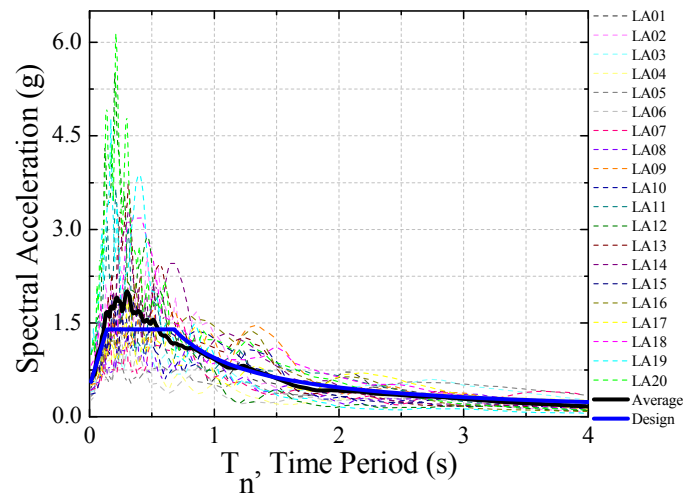


Figure 6. Response spectrum for 20 DBE level earthquakes and their average along with design spectrum

4 ANALYSIS RESULTS

The results of nonlinear push-over analysis and NTH analysis were extracted. The lateral strength, lateral stiffness, the yielding mechanism of the components for the lateral push, the base shear variation with the roof drift were extracted from the push-over analysis. The relative lateral displacement to the corresponding storey height is defined as the inter-storey drift ratio. From the non-linear time history analysis maximum and residual inter-storey drift ratios were studied. These results directly indicate the extent of damage to the frame system during the earthquake. Hence it is the measurement of the extent of retrofitting and reusability of the structures after the seismic excitation.

4.1 Push-over analysis

The push over analysis were carried out for all the frames. The base shear vs. roof drift were plotted for

both 3 storey and 6 storey frames separately. Fig. 7 (a) & (b) shows the base shear vs. roof drift of frames. Among the 3-storey buildings 3VCBFR6 showed a maximum elastic stiffness of 91546 kN/m and the least was showed by 3VBRBFR8 as 54393kN/m. The frames 3VBRBFR7, 3VHBFR8 and 3VHBFR7 showed an initial stiffness of 61068kN/m, 82313kN/m and 89535kN/m respectively. For the 6-storey frames the similar trend followed. The initial stiffness of 6VBRBFR8, 6VBRBFR7, 6VHBFR8, 6VHBFR7 and 6VCBFR6 were 22543 kN/m, 24838 kN/m, 32822 kN/m, 35093 kN/m and 40776 kN/m respectively. For 3-storey frames, up to a 4% roof drift the maximum lateral strength was 2743 kN for 3VCBFR6. 3VBRBFR8 and 3VHBFR8 showed lower values for the same as 2658kN and 2677kN in order. 3VBRBFR7 showed a maximum capacity of 3079kN and 3VHBFR7 showed a maximum capacity of 3059kN. The column yielding were observed in 3VCBFR6 at 0.4% roof drift. For all other 3-storey frames the column yielding were observed near to 1.5% of roof drift. For the 6-storey building the maximum lateral strength up to 4% push were 2462kN, 2837kN, 2468kN, 2846kN and 1112kN for 6VBRBFR8, 6VBRBFR7, 6VHBFR8, 6VHBFR7 and 6VCBFR6 respectively. The trend was same as the 3-storey building with maximum for 6VHBFR7 and least for 6VBRBFR8.

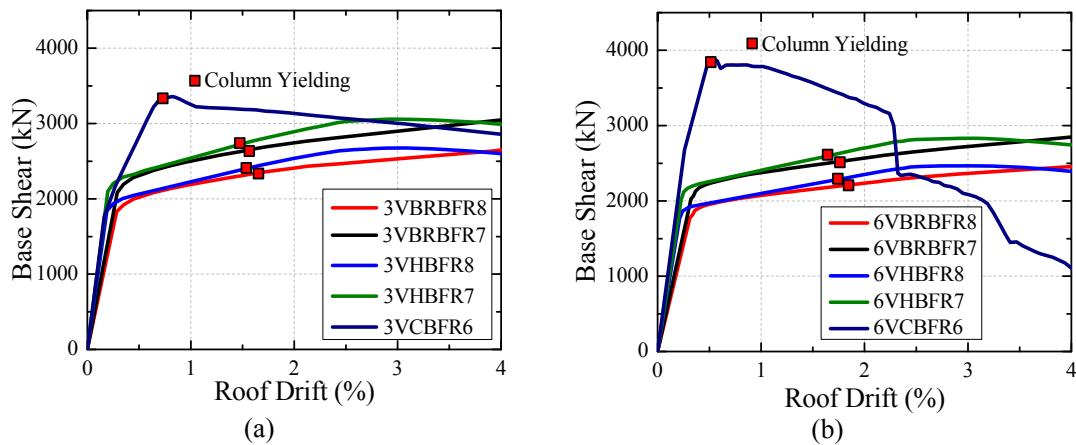


Figure 7. (a) Base shear vs. roof drift for 3 storey frames, (b) Base shear vs. roof drift for 6-storey

The column yielding for 6VCBFR6 was observed near to 0.5% roof drift and for all other 6-storey frames it was observed around 1.8% of roof drift. From the push over analysis the trend was such that when R value changed from 8 to 7 the system stiffness improved in the range of 7% to 12% and the strength as lateral capacity increased around 15 %. The improvement of initial stiffness form BRBF to HBF was in the range of 30% to 40%, but the lateral load capacity remained almost comparable. Further 6VCBFR6 at 2.2% roof drift there was a sharp degradation in the lateral strength due to buckling and yielding of all the braces with bottom column hinging. This degradation successively continued depending on the column hinging at different floor levels.

Table 2. Summary of push-over analysis results

	3-Storey Frame				
	3VCBFR6	3VBRBFR8	3VBRBFR7	3VHBFR8	3VHBFR7
Elastic Stiffness (kN/m)	91546	54393	61068	82313	89535
Strength at 4% Drift	2743 kN	2658 kN	3059 kN	2677 kN	3079 kN
	6-Story Frame				
	6VCBFR6	6VBRBFR8	6VBRBFR7	6VHBFR8	6VHBFR7
Elastic Stiffness (kN/m)	40776	22543	24838	32822	35093
Strength at 4% Drift	1112 kN	2462 kN	2837 kN	2468 kN	2846 kN

4.2 Inter-storey Drift Ratio (ISDR)

For the 20 ground motions in the DBE level, the average of maximum inter-storey drift ratio was plotted.

Fig. 8 (a) & (b) shows the ISDR of all the frames for DBE level earthquake. Among 3-storey frames maximum of the average maximum ISDR was given by 3VCBFR6 at first floor as 1.42%. For the same frame the value of ISDR for second and third floor were in the range of 0.90%. For all other frames the maximum ISDR was observed at second floor. Among the remaining frames the maximum of the maximum ISDR of 1.33% for 3VBRBFR8 and the least was 1.09% for 3VHBFR7 in their respective second floors. 3VBRBFR7 and 3VHBFR8 showed a maximum ISDR of 1.19% at the second floor level. The same trend was observed in 6-storey frames. Except for 6VCBFR6 all the frames showed a maximum ISDR at second floor level. And the former one showed a maximum ISDR at first floor as 1.56%. The maximum ISDR were 1.24%, 1.15%, 1.20% and 1.13% respectively for 6VBRBFR8, 6VBRBFR7, 6VHBFR8 and 6VHBFR7 in order. When the R value changes from 8 to 7, a percentage reduction in the range of 7% was obtained. The reduction in maximum ISDR from 6VBRBFR8 to 6VHBFR7 was around 10%. Table 3 summarizes the variation of ISDR.

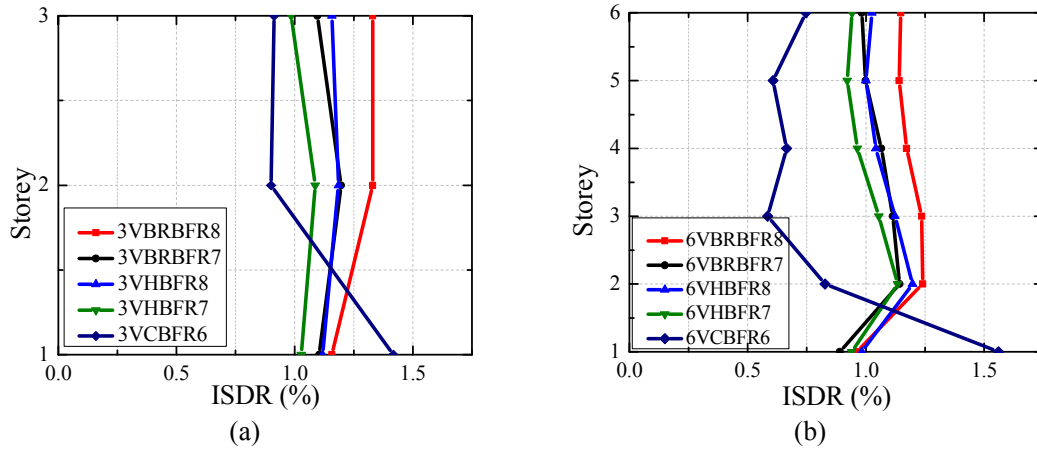


Fig. 8. DBE level drift response, (a) ISDR of 3-storey frames, (b) ISDR of 6-storey frames

Table 3. Summary of maximum inter-storey drift ratio response

3-Storey Frame					
	3VCBFR6	3VBRBFR8	3VBRBFR7	3VHBFR8	3VHBFR7
3 rd Storey	0.91	1.34	1.11	1.16	0.99
2 nd Storey	0.90	1.33	1.21	1.19	1.09
1 st Storey	1.42	1.16	1.10	1.12	1.03
6-Storey Frame					
	6VCBFR6	6VBRBFR8	6VBRBFR7	6VHBFR8	6VHBFR7
6 th Storey	0.75	1.15	0.98	1.03	0.94
5 th Storey	0.61	1.14	0.99	1.01	0.92
4 th Storey	0.67	1.17	1.07	1.04	0.97
3 rd Storey	0.59	1.23	1.12	1.12	1.06
2 nd Storey	0.83	1.24	1.14	1.19	1.14
1 st Storey	1.56	0.96	0.89	0.98	0.94

4.3 Residual Drift Ratio (RDR)

The main objective of this investigation was to limit the RDR to minimize the retrofitting difficulty. Among 3 storey buildings, 3VBRBFR8 showed the average maximum RDR of 0.48% at top floor level. The 3VBRBFR7 with improved R value showed 0.38% average maximum RDR at second floor. In the case of 3VHBFR8 and 3VHBFR7 the RDR maximum values were 0.25% and 0.20%. In both cases improvement in reducing the RDR is around 20% due to the shifting of R value from 8 to 7. The change from 3VBRBFR8 to 3VHBFR8 and from 3VBRBFR7 to 3VHBFR7 is in the range of 40% reduction

of average maximum RDR. For the 3VCBFR6 a maximum RDR of 0.36% was observed at first floor. Among 6-storey frames 6VBRBFR8 had a maximum RDR of 0.49% at fourth floor. For 6VBRBFR7 the maximum RDR was 0.41% at first floor, this was 16% less than the previous case. The maximum RDR for 6VHBF8 was 0.38% at third floor and it was 0.28% for 6VHBF7 at first floor level. This showed a percentage difference of 36%. Percentage reduction of maximum RDR for 6VHBF8 compared to 6VHBF7 was 32% and the reduction for 6VHBF7 compared to 6VBRBFR7 was around 30%. Overall change from 6VBRBFR8 to 6VHBF7 was around 42% reduction in the maximum RDR. 6VCBFR6 showed a maximum RDR of 0.36% at first floor. This was greater than the maximum RDR of 6VHBF7 (0.28%). Fig. 9 and Table 4 shows the variation of RDR for both 3 and 6 storey frames over the height.

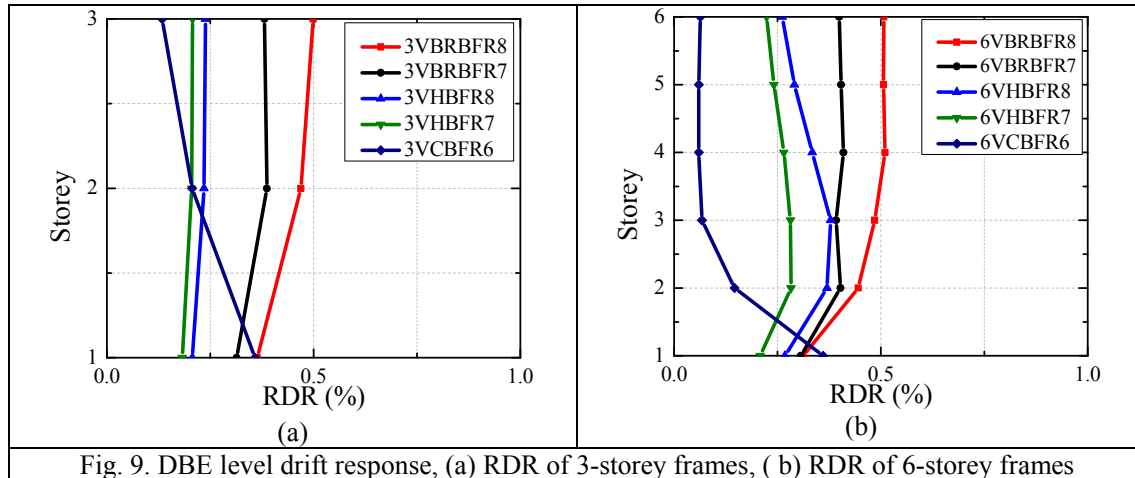


Fig. 9. DBE level drift response, (a) RDR of 3-storey frames, (b) RDR of 6-storey frames

Table 4. Summary of maximum residual drift ratio response

3-Storey Frame					
	3VCBFR6	3VBRBFR8	3VBRBFR7	3VHBF8	3VHBF7
3 rd Storey	0.13	0.49	0.38	0.24	0.21
2 nd Storey	0.21	0.47	0.39	0.23	0.20
1 st Storey	0.36	0.36	0.31	0.21	0.18
6-Storey Frame					
	6VCBFR6	6VBRBFR8	6VBRBFR7	6VHBF8	6VHBF7
6 th Storey	0.06	0.51	0.39	0.26	0.23
5 th Storey	0.05	0.50	0.40	0.29	0.24
4 th Storey	0.05	0.51	0.41	0.33	0.27
3 rd Storey	0.07	0.49	0.39	0.38	0.28
2 nd Storey	0.15	0.45	0.40	0.37	0.29
1 st Storey	0.36	0.31	0.30	0.27	0.21

5 SUMMARY OF THE STUDY

A hybrid brace with a combination of Short-Length Buckling Restrained Brace (SLBRB) and elastic Buckling Type Brace (BTB) segment has been proposed and the performance of such Hybrid Brace (HB) in a steel Hybrid Braced Frames (HBF) system with different R values were investigated analytically. The non-linear static and dynamic analysis were carried out for two different heights and the results were compared with equivalent CBF and BRBF. The proposed HB was very effective in reducing Residual Drift Ratio (RDR) of the frame systems compared to Buckling Restrained Braced Frames (BRBFs). The conclusions are listed below.

1. The introduction of the proposed hybrid in to the steel frames were successful in limiting both ISDR and RDR by improving the strength and stiffness of the framed system.
2. The improvement of initial stiffness in BRBFs or in HBFs by decreasing the R value from 8 to 7 is in the range of 7%-12%. The improvement of initial stiffness from BRBFs to HBFs (for same R value) is in the range of 40%.
3. The maximum reduction in peak ISDR from BRBFR8 to HBFR7 is in the range of 10%.
4. The percentage reduction in maximum RDR due to improvement of R value from 8 to 7 is in the range of 20%. And the reduction of the maximum RDR for the same change in HBFs was 30% compared to BRBFs.
5. The reduction of maximum RDR from BRBFR8 to HBFR 7 was in the range of 40%. And the maximum RDR of HBFs were less than the corresponding CBFs.
6. The yielding core-length for SLBRBs, ductility demand requirements of HBs and SLBRB-elastic BTB joint continuity in HBs needs further research to understand the complete behaviour of HBFs.

REFERENCES:

- American Institute of Steel Construction. 2010a. Seismic provisions of structural steel buildings. *ANSI/AISC 341-10*. Chicago: IL.
- American Institute of Steel Construction. 2010b. Specification for structural steel buildings. *ANSI/AISC 360-10*. Chicago: IL.
- American Society of Civil Engineers. 2010. Minimum design loads for buildings and other structures. *ASCE/SEI 7-10*. Reston: VA.
- Chao S. -H. Karki N. B. & Sahoo D. R. 2012. Seismic behaviour of steel building s with hybrid braced frames. *ASCE Journal of Structural Engineering*. 139 (6). 1019-1032.
- Computers Structures Inc, PERFORM-3D. 2013. User guide. *Version 5*. Berkeley: CA.
- Fahnestock L. A. Ricles J. M. & Suace R. 2007. Experimental evaluation of a large-scale buckling-restrained braced frame. *Journal of Structural Engineering*. 133 (9). 1205-1214.
- Federal Emergency Management Agency. 2000. NEHRP recommended provisions for seismic regulations for new buildings and other structures. *FEMA-356*. Washington: DC.
- Merritt S. Uang C. M. & Benzoni G. 2003. Sub-assembly testing of star seismic buckling restrained braces. *Rep. TR-2003/04*. Department of Structural Engineering, University of California. La Jolla: CA.
- Pandikkadavath M. S. & Sahoo D. R. 2014. Experimental study on reduced-length buckling restrained braces under slow cyclic loading. *10th National Conference on Earthquake Engineering (10NCEE), Anchorage, 21-25 July 2014*. Anchorage: Alaska
- Sabelli R. 2000. Research on improving the design and analysis of earthquake resistant steel braced frames. *FEMA/EERI Report*, Earthquake Engineering Research Institute. Oakland: CA.
- Sabelli R. Mahin S. & Chang C. 2003. Seismic demands on steel braced frame buildings with buckling-restrained braces. *Engineering Structures*. 25 (5). 655-666.
- Sahoo D. & Brown T. 2003. Behaviour of square hollow structural steel braces with end connections under reversed cyclic axial loading. *Canadian Journal of Civil Engineering*. 30 (4). 745-753.
- Shaback B. R. & Chao S. -H. 2010. Performance based plastic design method for buckling-restrained braces. *Engineering Structures*. 32 (9). 2950-2958.
- Somerville P.G. Smith M. Punyamurthala S. & Sun J. 1997. Development of ground motion time histories for phase 2 of the FEMA/SAC steel project. *FEMA/SAC, Rep. No. SAC/BD-97/04*. Sacramento: CA.
- Wu A.C. Lin P. C. & Tsai K. C. 2014. High-mode buckling response of buckling-restrained brace core plates. *Earthquake Engineering and Structural Dynamics*. 43. 373-393.